

Quintessence phase of the late-time Universe in $f(Q, T)$ gravity

Shambel Sahlua^{a,b}, Bhupendra Kumar Shukla^c, Rishi Kumar Tiwari^d, Değır Sofuođlu^{e,a},
Alnadhief H. A. Alfedeei^{f,g,a}

^aCentre for Space research, North-West University, Potchefstroom, 2520, North-West, South-Africa

^bDepartment of Physics, College of Natural and Computational Science, Wolkite University, Wolkite, Ethiopia

^cDepartment of Mathematics, Govt. College Bandri, Sagar, Madhya Pradesh, India

^dDepartment of Mathematics, Govt. Model Science College, Rewa, Madhya Pradesh, India

^eDepartment of Physics, Istanbul University, Vezneciler, Fatih, Istanbul, Turkey

^fDepartment of Mathematics and statistics, Imam Mohammad Ibn Saud Islamic University, Riyadh, Saudi Arabia

^gDepartment of Physics, Faculty of Science, University of Khartoum, P.O. Box 321, Khartoum, 11115, Sudan

Abstract

In this paper, we have studied the late-time accelerating expansion of the Universe using the matter-geometry coupled $f(Q, T)$ gravity model, where Q is the non-metricity scalar and T represents the trace of the energy-momentum tensor. We constrain the best-fit values of cosmological parameters Ω_{m0} , H_0 , α_0 and β_0 through the Monte Carlo Markov Chain (MCMC) simulation using 31 Hubble parameter data points from cosmic chronometers (CC) and 26 data points from baryon acoustic oscillations (BAO), making a total of 57 datasets (labeled CC+BAO), as well as SNIa distance moduli measurements from the Pantheon+ sample, which consists of 1701 light curves of 1550 distinct supernovae (labeled Pantheon +SHOES), and their combination (labeled CC+BAO+Pantheon +SHOES). We compare our constrained Hubble constant H_0 value with different late-time and early-time cosmological measurements. Deceleration parameter $q(z)$, effective equation of state parameters $w_{eff}(z)$, Hubble parameter $H(z)$, and distance modulus $\mu(z)$ are numerical results of dynamical quantities that show that the $f(Q, T)$ gravity model is compatible with a transition towards a quintessence-like phase in the late-time. In conformity with Λ CDM, we moreover take into account the geometrical interpretations by considering the state-finder parameters $r - s$ and $r - q$, which are crucial parameters for additional analysis. Additionally, the statistical analysis has been carried out for further investigation.

Keywords: $f(Q, T)$ cosmology, Quintessence Phase, State-finder

PACS: 04.50.Kd, 98.80.Jk, 98.80.-k, 95.36.+x, 98.80.Cq

¹corresponding author: sahlushambel@gmail.com

1. Introduction

Various observation measurements including Type Ia Supernovae [1, 2], together with large scale structure (LSS) [3, 4], Baryon Acoustic Oscillations (BAO) [5], and microwave background (CMB) anisotropies [6, 7] have been shown that the Universe has experienced for accelerating expansion due to the influence of dark energy (DE) which is an exotic component that produces negative pressure and drives late-time cosmic acceleration. DE makes up roughly 73% of the mass-energy budget of the Universe, while dark matter and regular baryonic matter make up 23% and 4%, respectively, according to the most recent measurements from the Planck satellite mission [8]. Numerous alternatives, including quintessence [9, 10], K-essence [11, 12], Chaplygin gas models [13, 14, 15], decaying vacuum models [16, 17, 18, 19], and others follow the characteristic of DE. In the last two decades, the modified gravity theories (MGT) have been suggested as an alternative to traditional cosmology and are gaining popularity for explaining the process of late-time cosmic acceleration without the need for a dark energy scenario. A few commonly used alternative MGTs including the matter-geometry coupling in the form of $f(R)$ gravity (R being the curvature scalar) [20, 21, 22], $f(T)$ gravity (\mathcal{T} being the torsion scalar) [23, 24, 25], $f(R, T)$ gravity [26], coupling of matter-curvature $f(R, L_m)$ (L_m being matter Lagrangian density) [27], $f(Q)$ gravity (Q being the non-metricity scalar), [28, 29], and matter-geometry coupling in the form of $f(Q, T)$ gravity (where T is the trace of stress energy-momentum tensor) [30]. Since it may handle several types of astrophysical and cosmological challenges, a matter-geometry coupling form of the $f(Q, T)$ gravity has drawn the attention of many astrophysicists and cosmologists [30, 31, 32] among all these geometric MGTs. For instance, the stress energy-momentum tensor T and the non-metricity scalar Q is used to define the gravitational Lagrangian, whose dependency may be caused by quantum phenomena or exotic imperfect fluids [33]. By changing the gravitational action about both metric and connection, the field equations were established. Without the need for DE, the matter-energy coupling in $f(Q, T)$ gravity plays a crucial part in providing a full theoretical account of the Universe's late-time cosmic acceleration. The energy conservation and phase-space analysis broadly discuss $f(Q, T)$ gravity as presented in [32]. According to Shiravand et al., [34], $f(Q, T)$ gravity has been suggested to provide an alternative viewpoint on the phenomenon of inflation in the early Universe. This theory can also naturally reproduce the observed power spectrum of cosmic microwave background radiation while addressing some of the flaws in the conventional inflationary paradigm [35].

The covariant formulation in $f(Q, T)$ gravity is critical for ensuring theoretical consistency, enabling exact energy conservation rules, facilitating dynamical investigation, and avoiding frame-dependent challenges. As presented in [36], the covariant formalism of $f(Q)$ gravity has been highlighted in the importance of avoiding the problem of gauge choice conflicts with the coordinate system it is chosen based on symmetry. The covariant formalism is a suitable non-vanishing affine connection for a given metric. In [32], the covariant formalism of $f(Q, T)$ gravity model extensively analyzes and handles phase space analysis. In this study, we use the covariant formalism to address the universe's accelerating expansion with various data sets.

The accelerating expansion of the universe has been explored within the $f(Q, T)$ gravity framework in studies such as [37, 38, 39, 40, 41, 42], using a specific parameter to derive the modified Hubble parameter. However, such assumptions add major biases that may undermine the model's effectiveness. We suggest that this method of describing cosmic dynamics is inco-

herent. In certain cases, the resulting Hubble parameter [37, 38, 42] due to the parametrization approach recovers neither GR nor the Λ CDM model, indicating a potential inconsistency in the parametrization approach. In this paper, we proposed a coherent functional form $f(Q, T) = -\alpha_0 Q - \beta_0 \frac{T^2}{H_0^2} + \eta_0$ (where $\alpha_0 \neq 0$, β_0 and η_0 are constants) which is the general form presented in [30], which show up the quintessence phase of the Universe. The best-fit values of the cosmological parameters are constrained by utilizing cosmological datasets, specifically, we use Type I Supernova distance moduli measurements from the Pantheon+SHOES [43], the measurements of Hubble parameter $H(z)$ which consists of 57 data points in total [44, 45], 31 data points from the relative ages of massive, early-time, passively-evolving galaxies, known as cosmic chronometers (CC) with 26 data points from the baryon acoustic oscillations (BAO). To evaluate the potential of the $f(Q, T)$ gravity model in addressing the H_0 tensions for upcoming works (Note that, the cosmological tension is beyond our current target of the work), we compared our H_0 values with i) early measurements, including Planck 2018 ($H_0 = 67.4 \pm 0.5$ km/s/Mpc) [46], Dark Energy Spectroscopy Instrument (DESI) ($H_0 = 68.4 \pm 1.0$ km/s/Mpc) [47], and BAO ($H_0 = 67.2 \pm 1.2$ km/s/Mpc) [48]; and ii) late-time measurements derived from direct observations of the local Universe, such as Supernovae and H_0 for the Equation of State (SHOES) ($H_0 = 73.0 \pm 1.3$ km/s/Mpc) [49], H0LiCOW ($H_0 = 73.3 \pm 1.8$ km/s/Mpc) [50], and Hubble Space Telescope (HST) $H_0 = 72.9 \pm 2.4$ km/s/Mpc [51]. The MCMC method is employed to systematically fit the model parameters α_0 , β_0 , H_0 , and Ω_{m0} to observational data. This approach provides probability distributions for each parameter, enhancing the accuracy of parameter estimation and enabling a strong comparison with the Λ CDM model. By analyzing the MCMC results, the model's compatibility with current observational data is evaluated, with parameter ranges that align with the known cosmic expansion history. In this context, we consider the MCMC likelihood contours with the 1σ and 2σ confidence intervals for the parameters. Then using the results of the MCMC analysis, we reconstruct our theoretical model with observational data. The Hubble parameter $H(z)$, the distance modulus $\mu(z)$, the deceleration parameter $q(z)$, and the effective equation of state parameter $\omega_{\text{eff}}(z)$ are discussed using their plots, along with diagnostics such as the state finder ($r - s$ and $r - q$ planes) and $Om(z)$ diagnostics, to determine the nature of expansion and dark energy in the model. The plots suggest a transition toward the Λ CDM fixed point, highlighting the model's evolution towards a cosmological constant-like behavior at late times, and indicating that the model aligns most closely with quintessence. The statistical analysis compares the $f(Q, T)$ gravity model with Λ CDM using the Akaike Information Criterion (AIC) and Bayesian Information Criterion (BIC), calculated for each dataset. While the $f(Q, T)$ model demonstrates some observational support, particularly in terms of the AIC values, the BIC results show a consistent preference for the Λ CDM model. Thus, the $f(Q, T)$ framework and the chosen model form not only provide a generalization of GR but also offer a more comprehensive approach to addressing the open questions of modern cosmology, including the transition between decelerating and accelerating phases of the Universe and the behavior of dark energy.

This paper is organized as follows: Section 2 provides the basic framework of $f(Q, T)$ gravity, including its field equations and relevant physical quantities. In this section, we present the chosen model form of $f(Q, T)$ and derive the modified Hubble parameter equation. Section 4 outlines the observational datasets and methods used to constrain the model parameters, including the Hubble, Pantheon+SHOES, and BAO datasets. Section 4 includes a statistical analysis that compares the $f(Q, T)$ model with Λ CDM using AIC and BIC to assess the

model's observational support. We also analyze the model's cosmographic parameters and apply geometrical diagnostics, such as the $r - s$ and $r - q$ state finder parameters and the $Om(z)$ diagnostic. Finally, in Section 5, we present the results, discuss our findings, and conclude the study.

2. The $f(Q, T)$ cosmology

The modified theory of gravity $f(Q, T)$ fundamental equations are outlined in this section. We begin by applying the $f(Q, T)$ gravitational action, which was first proposed by [30], as follows:

$$S = \int \left[\frac{1}{2\kappa} f(Q, T) + L_M \right] \sqrt{-g} d^4x. \quad (1)$$

Here

$$Q = -g_{\mu\nu} \left(L_{\mu\beta}^\alpha L_{\nu\alpha}^\beta - L_{\beta\alpha}^\alpha L_{\mu\nu}^\beta \right),$$

is a non-metricity scalar, and

$$L_{\beta\gamma}^\alpha = -\frac{1}{2} g^{\alpha\lambda} \left(\nabla_\gamma g_{\beta\lambda} + \nabla_\beta g_{\lambda\gamma} - \nabla_\lambda g_{\beta\gamma} \right),$$

is the disformation tensor, T is trace of the energy-momentum tensor $T_{\mu\nu}$, L_m is the Lagrangian matter density, and g is determinant of the metric tensor $g_{\mu\nu}$.

The covariant formulation of the gravitational field equations in $f(Q, T)$ theory of gravity is obtained by varying the action in (1) with respect to the metric tensor $g_{\mu\nu}$, as

$$-\frac{2}{\sqrt{-g}} \nabla_\alpha (f_Q \sqrt{-g} P^\alpha_{\mu\nu}) - \frac{1}{2} f g_{\mu\nu} + f_T (T_{\mu\nu} + \Theta_{\mu\nu}) - f_Q (P_{\mu\alpha\beta} Q_\nu^{\alpha\beta} - 2Q_{\mu\alpha}^{\alpha\beta} P_{\beta\nu}) = \kappa T_{\mu\nu}, \quad (2)$$

Where

$$\Theta_{\mu\nu} = g^{\alpha\beta} \frac{\delta T_{\alpha\beta}}{\delta g^{\mu\nu}}, \quad f_Q = \frac{\partial f(Q, T)}{\partial Q}, \quad f_T = \frac{\partial f(Q, T)}{\partial T}, \quad (3)$$

and

$$P^\alpha_{\mu\nu} = -\frac{1}{2} L_{\mu\nu}^\alpha + \frac{1}{4} (Q^\alpha - \widehat{Q}^\alpha) g_{\mu\nu} - \frac{1}{4} \delta_{(\mu}^\alpha Q_{\nu)}, \quad (4)$$

$$Q_{\lambda\mu\nu} = -\frac{\partial g_{\mu\nu}}{\partial x^\lambda} + g_{\nu\sigma} \widehat{\Gamma}_{\mu\lambda}^\sigma + g_{\sigma\mu} + g_{\sigma\mu} \widehat{\Gamma}_{\nu\lambda}^\sigma. \quad (5)$$

Symmetric teleparallel gravity is equivalent to general relativity. This equivalence can easily be proven in the so called coincident gauge, for which [30]

$$\widehat{\Gamma}_{\mu\nu}^\lambda \equiv 0. \quad (6)$$

The variation of the action (1) with respect to the connection can be performed while imposing two constraints, $R_{\beta\mu\nu}^\alpha = 0$ and $T_{\mu\nu}^\alpha = 0$, and using the Lagrange multiplier method. Consequently, the corresponding FEs are

$$\nabla_\mu \nabla_\nu (2\sqrt{-g} f_Q P_{\mu\nu}^\alpha + \kappa H_\alpha^{\mu\nu}) = 0, \quad (7)$$

where $H_\alpha^{\mu\nu}$ is the hyper-momentum tensor density defined as

$$H_\alpha^{\mu\nu} \equiv \frac{f_T \sqrt{-g}}{2\kappa} \frac{\delta T}{\delta \Gamma^\alpha{}_{\mu\nu}} + \frac{\delta(\sqrt{-g}L_m)}{\delta \Gamma^\alpha{}_{\mu\nu}}. \quad (8)$$

We present the eagerly anticipated covariant version of the $f(Q, T)$ theory in this section. To learn more about the application of covariant derivative, one must refer to [32, 36]. First, we will look at the restrictions that are free of curvature and torsion.

$$\mathring{R}_{\mu\nu} + \mathring{\nabla}_\alpha L^\alpha{}_{\mu\nu} - \mathring{\nabla}_\nu \tilde{L}_\mu + \tilde{L}_\alpha L^\alpha{}_{\mu\nu} - L_{\alpha\beta\nu} L^{\beta\alpha}{}_\mu = 0, \quad (9)$$

$$\mathring{R} + \mathring{\nabla}_\alpha (L^\alpha - \tilde{L}^\alpha) - Q = 0. \quad (10)$$

Upon choosing the coinciding gauge in which $\Gamma^\lambda{}_{\mu\nu} = 0$ or $\mathring{\Gamma}^\lambda{}_{\mu\nu} = -L^\lambda{}_{\mu\nu}$. Then

$$\partial_\lambda \sqrt{-g} = -\sqrt{-g} \tilde{L}_\lambda. \quad (11)$$

Additionally, we obtain

$$\begin{aligned} \frac{2}{\sqrt{-g}} \partial_\lambda (\sqrt{-g} f_Q P^\lambda{}_{\mu\nu}) + f_Q (P_{\nu\rho\sigma} Q_\mu{}^{\rho\sigma} - 2P_{\rho\sigma\mu} Q^{\rho\sigma}{}_\nu) \\ = 2(\nabla_\lambda f_Q) P^\lambda{}_{\mu\nu} + 2f_Q (\mathring{\nabla}_\lambda P^\lambda{}_{\mu\nu} - L_{\alpha\beta\mu} P^{\beta\alpha}{}_\nu - L_{\alpha\beta\nu} P_\nu{}^{\beta\alpha} + L_{\nu\alpha\beta} P^{\alpha\beta}{}_\mu) \\ = 2(\nabla_\lambda f_Q) P^\lambda{}_{\mu\nu} + 2f_Q (\mathring{\nabla}_\lambda P^\lambda{}_{\mu\nu} - \tilde{L}_\alpha L^\alpha{}_{\nu\mu} + L_{\alpha\beta\nu} L^{\beta\alpha}{}_\mu). \end{aligned} \quad (12)$$

With the use of Eqs. (4), (9) and (10), we get

$$\begin{aligned} 2\mathring{\nabla}_\alpha P^\alpha{}_{\mu\nu} &= -\mathring{\nabla}_\alpha L^\alpha{}_{\mu\nu} + \frac{\mathring{\nabla}_\alpha (L^\alpha - \tilde{L}^\alpha)}{2} g_{\mu\nu} + \frac{\mathring{\nabla}_\nu \tilde{L}_\mu + \mathring{\nabla}_\mu \tilde{L}_\nu}{2} \\ &= \mathring{R}_{\mu\nu} + \frac{Q - \mathring{R}}{2} g_{\mu\nu} + \tilde{L}_\alpha L^\alpha{}_{\mu\nu} - L_{\alpha\beta\nu} L^{\beta\alpha}{}_\mu. \end{aligned} \quad (13)$$

The combination of (12)–(13) gives

$$\frac{2}{\sqrt{-g}} \partial_\lambda (\sqrt{-g} f_Q P^\lambda{}_{\mu\nu}) + f_Q (P_{\nu\rho\sigma} Q_\mu{}^{\rho\sigma} - 2P_{\rho\sigma\mu} Q^{\rho\sigma}{}_\nu) = 2(\nabla_\lambda f_Q) P^\lambda{}_{\mu\nu} + f_Q \left(\mathring{R}_{\mu\nu} - \frac{\mathring{R} - Q}{2} g_{\mu\nu} \right). \quad (14)$$

Lastly, the metric field equation can be covariantly recast as

$$f_Q \mathring{G}_{\mu\nu} + \frac{1}{2} g_{\mu\nu} (Q f_Q - f) + f_T (T_{\mu\nu} + \Theta_{\mu\nu}) + 2(\nabla_\lambda f_Q) P^\lambda{}_{\mu\nu} = \kappa T_{\mu\nu} \quad (15)$$

where $\mathring{G}_{\mu\nu}$ is the Einstein tensor corresponding to the Levi-Civita connection. Then, the effective stress energy tensor is defined as

$$\kappa T_{\mu\nu}^{\text{eff}} = \kappa T_{\mu\nu} - f_T (T_{\mu\nu} + \Theta_{\mu\nu}) - \frac{1}{2} g_{\mu\nu} (Q f_Q - f) - 2(f_{QQ} \nabla_\lambda Q + f_{QT} \nabla_\lambda T) P^\lambda{}_{\mu\nu}. \quad (16)$$

Where

$$\Theta_{\mu\nu} = p g_{\mu\nu} - 2T_{\mu\nu}. \quad (17)$$

We also assume the spatially homogeneous and isotropic FLRW metric

$$ds^2 = -dt^2 + a^2(t)(dx^2 + dy^2 + dz^2), \quad (18)$$

where $a(t)$ is the scale factor. The energy-momentum tensor of a perfect fluid is:

$$T_{\mu\nu} = (\rho + p)u_\mu u_\nu + pg_{\mu\nu}, \quad (19)$$

where the fluid's energy density, pressure, and four-velocity are denoted by ρ , p , and u_μ respectively. The nonmetricity scalar is obtained to be $Q = -6H^2$ in an adjusted coordinate system, and the trace of EMT $T = 3p - \rho$, or the Cartesian coordinates in the spatial variables of the line element (18) in which the connection is zero (the coincident gauge). From the modified field equations [30], the dynamical quantities are as follows:

$$\kappa\rho = \frac{f}{2} - 6f_Q H^2 - \frac{2f_T}{\kappa + f_T} (\dot{f}_Q H + f_Q \dot{H}), \quad (20)$$

and

$$\kappa p = -\frac{f}{2} + 6f_Q H^2 + 2(\dot{f}_Q H + f_Q \dot{H}). \quad (21)$$

The modified Friedman field equation can be written as:

$$3H^2 = \frac{f}{4f_Q} - \frac{1}{2f_Q} [(\kappa + f_T)\rho + f_T p], \quad (22)$$

and the acceleration equation becomes

$$2\dot{H} + 3H^2 = \frac{f}{4f_Q} - \frac{2\dot{f}_Q H}{f_Q} + \frac{1}{2f_Q} [(\kappa + f_T)\rho + (2\kappa + f_T)p]. \quad (23)$$

Having known the functional form of $f(Q, T)$ one can study the cosmological implications of the model. As mentioned earlier, we consider the power-law $f(Q, T)$ gravity model, $f(Q, T) = -\alpha_0 Q - \frac{\beta_0}{H_0^2} T^2 + \eta_0$. The term first term $-\alpha_0 Q$ plus the last term resembles the standard form of λ CDM, while the additional terms involving T allow for modifications that can address the Universe's late-time acceleration. For the case of $\alpha = 1, \beta = 0 = \eta_0$, the model exactly recovers to GR . One of the key advantages of using this particular form is that it enables the derivation of testable predictions that can be constrained using observational datasets. By fitting these datasets, the free parameters can be determined, allowing the model to be directly compared with observational evidence. Moreover, the additional T^2 term introduces non-trivial interactions between matter and geometry, which could lead to new insights into the nature of cosmic expansion. Using this particular model Eqs. (22), the modified Hubble parameter yield as

$$H = H_0 \sqrt{\frac{\Omega_{m0}(1+z)^3}{\alpha_0} + \frac{15\beta_0}{2\alpha_0} \Omega_{m0}^2 (1+z)^6 - \frac{\eta_0}{6\alpha_0}}. \quad (24)$$

At current time, where $z = 0$, equation (26) provides

$$1 - \frac{\Omega_{m0}}{\alpha_0} - \frac{15\beta_0}{2\alpha_0} \Omega_{m0}^2 = -\frac{\eta_0}{6\alpha_0} \quad (25)$$

and the normalized Hubble parameter becomes

$$h(z, \Omega_{m0}, \alpha_0, \beta_0) = \sqrt{\frac{\Omega_{m0}}{\alpha_0} ((1+z)^3 - 1) + \frac{15\beta_0}{2\alpha_0} \Omega_{m0}^2 ((1+z)^6 - 1) + 1} \quad (26)$$

Finally, the Λ CDM model is recovered when $\alpha_0 = 1, \beta_0 = 0$, vis

$$H^2 = H_0^2 [\Omega_{m0}(1+z)^3 + 1 - \Omega_{m0}] \quad (27)$$

The free parameters that will be constrained using the observational data are $\mathbf{p} = \mathbf{p}(\alpha_0, \beta_0, H_0, \Omega_{m0})$. For this model, the deceleration parameter, q is given by

$$q(z) = -1 + (1+z) \frac{1}{h} \frac{dh}{dz} \quad (28)$$

and the effective equation of state of the Universe components is

$$w_{eff}(z) = -\frac{1}{3} + \frac{2}{3}q(z). \quad (29)$$

The above equations (28) and (29), describe how the deceleration and effective EoS parameters evolve as functions of redshift, capturing the transition from a decelerating to an accelerating Universe. Latter we will discuss the numerical results. The generalized form of the distance modules $\mu(z)$ in Mpc yield as

$$\mu(z) = 25 + 5 \times \log_{10}(1+z) 300 \bar{h}^{-1} \int_0^z \frac{cdz'}{h(z')}, \quad \text{where } \bar{h} = H_0/100 \quad (30)$$

The dynamical parameters $h(z)$, $q(z)$, w_{eff} , and $\mu(z)$ are influenced by the values of β_0 and α_0 , which are essential parameters for studying cosmic evolution. In our $f(Q, T)$ gravity model, the cosmic evolution is affected by these parameters, leading to the following observations: i) The model exhibits nonphysical behavior when $\alpha_0 = 0$. ii) For $0 < \alpha_0 \ll 1$, the deceleration parameter $q(z) \geq 0$, indicates that the Universe is dominated by matter and will eventually collapse rather than accelerate. In contrast, when $\alpha_0 \gg 1$, dark energy dominates, resulting in an accelerated expansion of the Universe. iii) As α_0 approaches one, the model tends to align closely with late-time cosmology as described by the Λ CDM model. iv) If β_0 is significantly positive, dark matter dominates, explaining the early Universe where anisotropy was present. However, if $\beta_0 \ll 0$, dark energy becomes dominant in the past, leading to rapid early acceleration, which contradicts current cosmological understanding. v) For small values of $|\beta_0|$, the model may accurately describe the late-time quintessence phase of cosmic expansion. For our analysis, we have set the priors $\alpha_0 = [0.95, 1.20]$ and $\beta_0 = [-0.02, 0.02]$. For detailed analysis, the constraining parameters are presented in the upcoming section to find the best-fit values of α_0 and β_0 using different measurements.

3. Observational constraints

The three distinct observational datasets are the CC+BAO, Pantheon+SHOES, and their combination CC+BAO+Pantheon+SHOES datasets. In this work, we use various software and Python packages, including EMCEE [52, 53] and GetDist [54] to constrain the model parameters, namely: Ω_m, H_0, α_0 , and β_0 using these cosmological datasets.

3.1. Hubble datasets

We analyze the Hubble parameter $H(z)$ measurements using the theoretical models from Eq. (26) with observational Hubble parameter data, which include a total of 57 data points [44, 45]. This comprises of 31 data points derived from the relative ages of massive, early-time, passively-evolving galaxies, known as cosmic chronometers (CC), and 26 data points from BAO provided by the Sloan Digital Sky Survey (SDSS), Data Release 9 & 11 (DR9 and DR11), covering the redshift range $0.0708 < z \leq 2.36$. This dataset is referred to as CC+BAO. To determine the mean values of the model parameters, we employ the chi-square function, expressed as:

$$\chi_H^2(\mathbf{p}) = \sum_{i=1}^{57} \frac{[H_{th}(\mathbf{p}, z_i) - H_{obs}(z_i)]^2}{\sigma_{H(z_i)}^2} .$$

The Hubble parameter's hypothetical and observed values are represented in the calculation described above by the numeric values H_{th} and H_{obs} , respectively. The term $\sigma_{H(z_i)}$ refers to the standard deviation of the observed value of H .

3.2. Pantheon+SHOES datasets

One notable dataset included in this work is the Pantheon+SHOES dataset, which contains 1701 type Ia supernovae that passed spectroscopic confirmation. Supernovae with redshifts ranging from 0.01 to 2.3 were present in the Pantheon+SHOES samples. The luminosity distance can be calculated with this dataset. The general form of distance modulus $\mu(z)$ for the three $f(Q)$ gravity models become

$$\mu(z) = 25 + 5 \log_{10} D_L(z) , \quad (31)$$

where $D_L(z)$ is luminosity distance

$$D_L(z) = (1+z)300\bar{h}^{-1} \int_0^z \frac{cdz'}{h(z')^\gamma} \quad (32)$$

here $100\bar{h} = H_0$, and $D_L(z)$ is measure in Mpc.

$$\chi_{SN}^2(\mathbf{p}) = \sum_{i=1}^{1701} \frac{[\mu_{th}(\mathbf{p}, z_i) - \mu_{obs}(z_i)]^2}{\sigma_{\mu(z_i)}^2} . \quad (33)$$

3.3. Joint analysis

In this analysis, we have considered the combinations of the above datasets namely CC+BAO +Pantheon+SHOES for further model constraining. We also calculate the total minimum χ^2 as

$$\chi_{total}^2 = \chi_{SN}^2(\mathbf{p}) + \chi_H^2(\mathbf{p}) . \quad (34)$$

The MCMC likelihood contours at 1σ and 2σ originating from the CC+BAO+Pantheon+SHOES dataset are presented in Fig. 1 for illustrative purpose. As presented in Table 1, we provide the best-fit cosmological parameters for both the Λ CDM and $f(Q, T)$ gravity models across three datasets. Both models approach the Supernova measurement H_0 estimate (around 73 ± 1.3 km/s/Mpc) [49] when using the combined dataset, with Λ CDM reaching 74.01 ± 0.2 km/s/Mpc and $f(Q, T)$ at 72.88 ± 0.30 km/s/Mpc. Therefore, the $f(Q, T)$ gravity model provides a somewhat better alleviation of the Hubble tension based on late-time cosmological measurements. The detailed comparison is made in figure 6 with different observations.

Model/Data	Ω_{m0}	H_0	α_0	β_0
Λ CDM				
CC+BAO	$0.266^{+0.015}_{-0.018}$	$70.105^{+1.600}_{-1.600}$	-	-
Pantheon+SHOES	$0.284^{+0.013}_{-0.013}$	$71.86^{+1.300}_{-1.300}$	-	-
CC+BAO+Pantheon+SHOES	$0.24^{+0.060}_{-0.060}$	$74.01^{+0.200}_{-0.200}$	-	-
$f(Q, T)$ gravity model			α_0	β_0
CC+BAO	$0.275^{+0.015}_{-0.05}$	$69.70^{+1.82}_{-1.82}$	$1.101^{+0.006}_{-0.006}$	$-0.00072^{+0.0001}_{-0.0001}$
Pantheon+SHOES	$0.33^{+0.023}_{-0.023}$	$73.06^{+0.21}_{-0.21}$	$1.009^{+0.007}_{-0.007}$	$-0.00093^{+0.00084}_{-0.00084}$
CC+BAO+Pantheon+SHOES	$0.255^{+0.011}_{-0.011}$	$72.88^{+0.30}_{-0.30}$	$1.025^{+0.0015}_{-0.0015}$	$-0.00104^{+0.00054}_{-0.00047}$

Table 1: The calculated best-fit values for both the Λ CDM and the $f(Q, T)$ gravity models using CC+BAO, Pantheon+SHOES, and CC+BAO+Pantheon+SHOES datasets.

Model/Data	$\mathcal{L}(\hat{\theta} data)$	χ^2	χ^2_ν	AIC	$ \Delta AIC $	BIC	$ \Delta BIC $
Λ CDM							
CC+BAO	-16.327	32.655	0.593	36.655	0.0	40.741	0.0
Pantheon+SHOES	-374.520	-749.040	0.990	-753.040	0.0	763.917	0.0
CC+BAO+Pantheon+SHOES	-428.780	857.560	0.986	861.560	0.0	872.503	0.0
$f(Q, T)$ gravity model							
CC+BAO	-15.996	31.501	0.581	39.501	2.845	47.673	6.932
Pantheon+SHOES	-371.210	742.420	0.992	750.420	1.160	772.175	8.257
CC+BAO+Pantheon+SHOES	-425.240	850.480	0.986	858.480	3.070	880.367	7.863

Table 2: We present the calculated values of $\mathcal{L}(\hat{\theta}|data)$, χ^2 , χ^2_ν , AIC, $|\Delta AIC|$, BIC and $|\Delta BIC|$, for both the Λ CDM model and the $f(Q, T)$ gravity models using CC+BAO, Pantheon+SHOES, and CC+BAO+Pantheon+SHOES datasets.

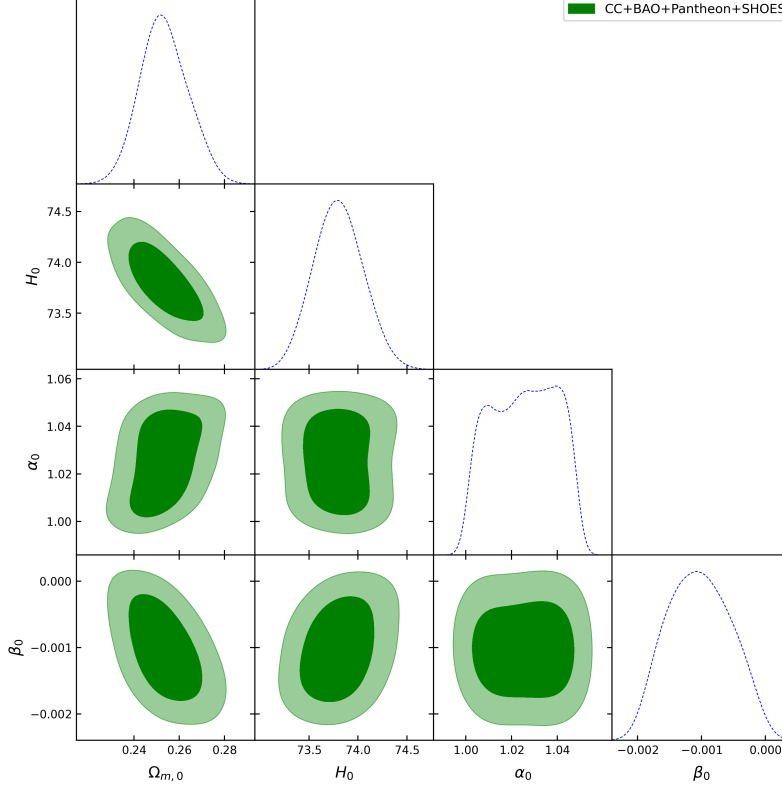


Figure 1: This plot illustrate the MCMC likelihood contours at 1σ and 2σ that originated from the CC+BAO+Pantheon+SHOES datasets.

Its H_0 estimate is the nearest to the distance ladder value, suggesting a partial resolution of the tension, though it remains below the expected $73 \pm 1.3 \text{ km/s/Mpc}$. The numerical results of $q(z)$, $w_{\text{eff}}(z)$, $H(z)$ and $\mu(z)$ are presented (see Figures 3 and 4) using the best-fit values of the parameter $\{\Omega_{m0}, H_0, \alpha_0, \beta_0\}$ taken from Table 1. For instance, the deceleration parameter $q(z)$ and the effective equation of state parameter $\omega_{\text{eff}}(z)$ are presented in Fig. 3 taken from equations (28) and (29) within the considered model. Figure 3 demonstrates the $f(Q, T)$ gravity model's alignment with the observed cosmic acceleration and its behavior relative to Λ CDM predictions under the constrained parameters. The deceleration parameter, $q(z)$ in the left panel of Fig. 3, describes the rate of change of the cosmic expansion history. In cosmological models, this parameter is crucial for understanding the transition from the early decelerating phase of the Universe to the current accelerating phase, which is attributed to dark energy. From the result, we notice the higher deviation between the $f(Q, T)$ gravity and Λ CDM model at higher redshifts. Since the $f(Q, T)$ gravity model indicates that the matter component becomes dominated at higher redshift slowing down the cosmic acceleration whereas at lower redshift, the model explains the dark energy that leads the cosmic acceleration. The effective equation of state (EoS) parameter, $w_{\text{eff}}(z)$ presented in the right panel of Fig. 3, characterizes the relationship between the pressure and density of the Universe's components, providing insights into the behavior of dark energy and

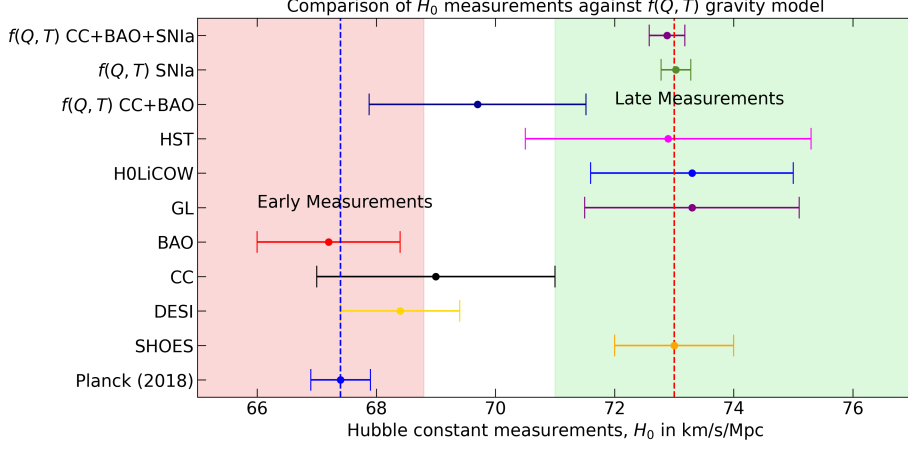


Figure 2: A comparison of late time H_0 using using different measurements with the corresponding values of H_0 for $f(Q, T)$ gravity model using CC+BAO, Pantheon+SHOES and CC+BAO+Pantheon+SHOES datasets.

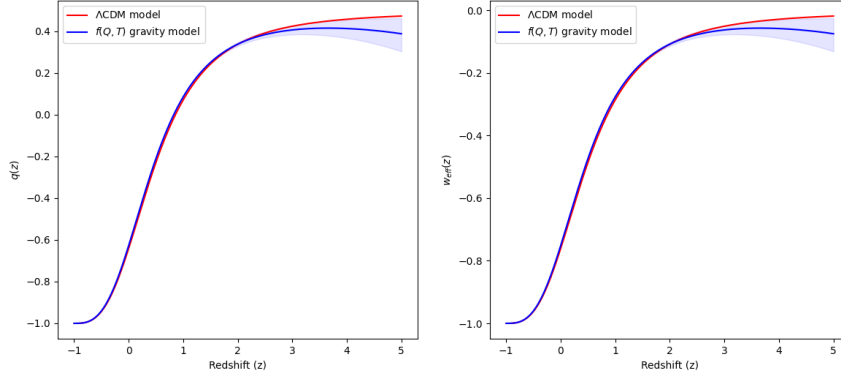


Figure 3: The deceleration parameter $q(z)$ (left panel) and the the effective equation of state parameter (right panel) for Λ CDM and $f(Q, T)$ gravity models. For illustrative purposes, the values of the constraining parameters Ω_{m0} , H_0 , α_0 and β_0 are taken from Table 1 using CC+BAO+Pantheon+SHOES datasets.

its role in cosmic acceleration. An EoS parameter value of $w_{\text{eff}} \approx -0.72$ at $z = 0$ corresponds to dark energy behaviors such as the quintessence phase. The evolution of $w_{\text{eff}}(z)$ over redshift can therefore help determine whether the model aligns with Λ CDM or suggests alternative dynamics in explaining cosmic acceleration. Furthermore, the Hubble and distance modulus diagram is also presented as presented in Fig 4 since these diagrams are crucial for studying the history of the Universe's expansion and help constrain the nature and strength of dark energy.

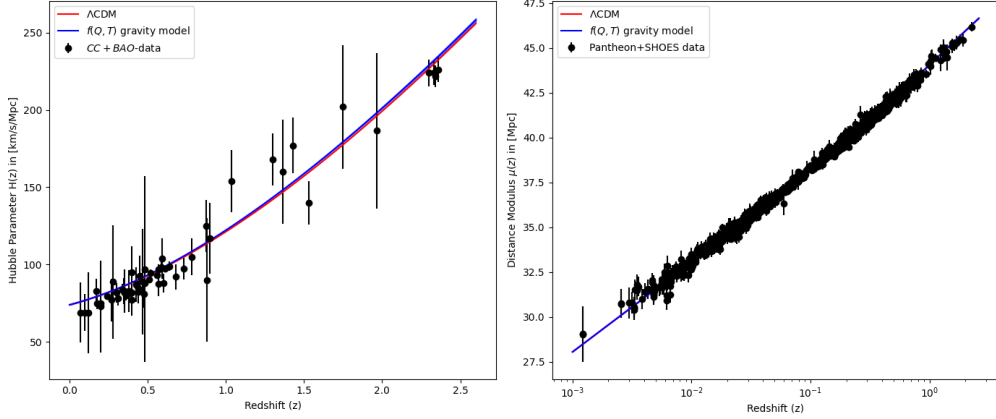


Figure 4: The Hubble parameter diagram $H(z)$ (left panel) and the distance modulus diagram (right panel) for Λ CDM and $f(Q, T)$ gravity models. For illustrative purposes, the values of the constraining parameters Ω_{m0} , H_0 , α_0 and β_0 are taken from Table 1 using CC+BAO+Pantheon+SHOES datasets.

4. Geometrical Interpretation

The acceleration of cosmic expansion is defined by the parameter $q(z)$, whereas the state finder parameter quantifies how far it deviates from a pure powerlaw behaviour. In comparison to other cosmological variables like the EoS parameter and the distance-redshift relation, the state finder analysis performs better. It is a geometrical diagnostic that does not presuppose the cosmological theory it is testing. Second, it is a model-independent method for differentiating between different dark energy (DE) scenarios, including the Λ CDM (Lambda Cold Dark Matter), SCDM (Standard Cold Dark Matter)[1, 55], HDE (Holographic Dark Energy) [56], CG (Chaplygin Gas) [13, 14], and quintessence [9, 10, 55]. Last but not least, it can be used to check the presumptions established by other cosmological parameters. Aside from the state finder parameters, the Om diagnostic allows us to further investigate the nature of the dark energy component and the model's behavior relative to Λ CDM and provides a more comprehensive understanding of the Universe's expansion dynamics. Here, we consider these two diagnostics which are commonly applied in cosmology.

4.1. $r - s$ and $r - q$ diagnostics

Statefinder analysis is a cosmological tool developed to assess the dynamics of the Universe by providing a model-independent method to differentiate between various dark energy (DE) models. The parameters for the state finder, r and s , are as follows [57]:

$$r = q(2q + 1) - \frac{\dot{q}}{H} \quad \text{and} \quad s = \frac{(r - 1)}{3(q - \frac{1}{2})}. \quad (35)$$

This approach uses the Hubble parameter and its temporal derivatives to form the statefinder parameters r and s , which offer a geometrical diagnostic that does not rely on specific assumptions about the underlying cosmological theory. The statefinder technique, introduced as an extension of the equation of state (EoS) parameter $w_{eff}(z)$, quantifies deviations from pure power-law expansion, providing more detailed insights into the nature of cosmic acceleration. Unlike

traditional cosmological variables such as the EoS parameter or the distance-redshift relation, statefinder analysis performs better in distinguishing between different DE models, including Λ CDM for $r = 1, s = 0$, SCDM for $r = 1, s = 1$ [57], HDE (Holographic Dark Energy) for $r < 1, s > 0$ [56], Chaplygin Gas (CG) for $r > 1, s < 0$ [13, 14], and quintessence for $r < 1, s > 0, r < 1$ [9, 10]. Furthermore, it can be used to validate the assumptions made by other cosmological parameters, offering a more robust tool for probing the nature of dark energy and the acceleration of the Universe. In this context, the $r - q$ plane is particularly useful in visualizing the evolutionary trajectory of the Universe and distinguishing between various cosmological models. The deceleration parameter q , which describes the rate of change in the cosmic expansion, is combined with the statefinder parameter r , allowing a more detailed analysis of the Universe's transition from deceleration to acceleration. Different DE models trace distinct paths in the $r - q$ plane, making it a valuable diagnostic tool. For instance, the fixed point ($r = 1, q = 0.5$) corresponds to the standard matter-dominated phase, while the point ($r = 1, q = -1$) indicates a de Sitter Universe dominated by a cosmological constant. By examining the trajectory of a given model in the $r - q$ plane, one can assess whether the model follows a path consistent with known cosmic history, including the transition from decelerating to accelerating expansion. This makes the $r - q$ plane an essential component of statefinder analysis, complementing the insights gained from the $r - s$ plane. For each of the datasets, Fig. (4.1) illustrates the trajectory of the model in the $r - s$ and $r - q$ plane. Given that the trajectory is in the region where $r < 1$ and $s > 0$, our model follows the quintessence scenario. The trajectory of our model indicates that the Universe will continue to expand at an accelerating rate as it approaches the Λ CDM fixed point in the future. This behavior is in agreement with recent data and gives support to the concept that acceleration is being driven by DE, which is symbolized by the cosmological constant. Additionally, it is evident from the $r - q$ graph in Figure 4 that the deceleration parameter will keep getting smaller over time and eventually approach a value of $q = -1$, which denotes a change from acceleration to a period of continuous expansion. A variety of observational data supports this transition, known as the De-Sitter phase ($r = 1$ and $q = -1$), which is a key component of contemporary cosmological models.

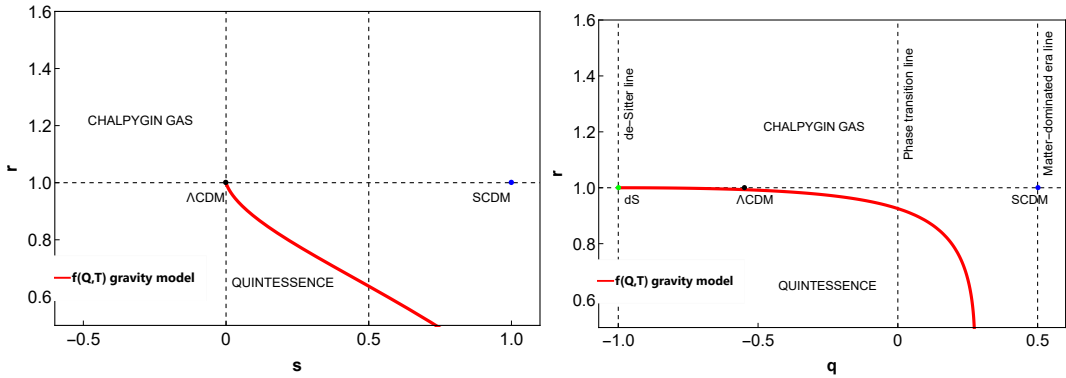


Figure 5: $r - s$ and $r - q$ planes.

4.2. Om diagnostic

The Om diagnostic is another valuable cosmological tool used to differentiate between various DE models by comparing the Hubble parameter $H(z)$ at different redshifts. $Om(z)$ is defined as

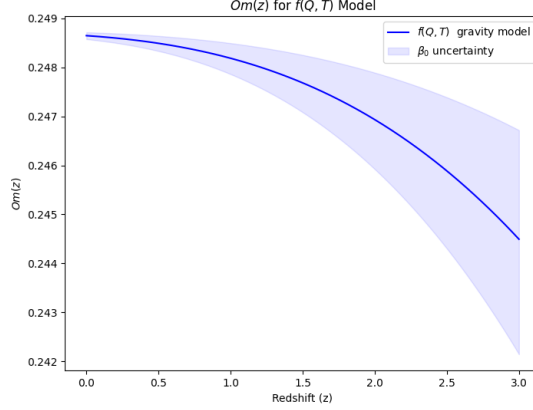


Figure 6: $Om(z)$ Vs z .

[58]

$$Om(z) = \frac{\left[\frac{H(z)}{H_0}\right]^2 - 1}{(1+z)^3 - 1}. \quad (36)$$

It provides a model-independent method to test the nature of DE and the expansion history of the Universe. Unlike the equation of state parameter w_{eff} , which requires assumptions about the underlying cosmological model, the Om diagnostic is directly based on observational data and offers a more straightforward interpretation. Accordingly, in Λ CDM model $Om(z)$ curve is constant, which means $Om(z)$ has no variation with redshift. If $Om(z)$ decreases with redshift z , then the DE model is quintessence[9, 10, 55]., and if $Om(z)$ increases with z , then the model is phantom, the $f(Q, T)$ gravity explains the quintessence phase of the late time Universe. Figure 5 represents the $Om(z)$ curve for our model. We see that the model approaches Λ CDM from the present to the future, as $Om(z)$ changes very little over this interval, eventually remaining almost constant, confirming the information obtained by the $r - s$ and $r - q$ tests.

4.3. Statistical analysis

Statistical values for both the Λ CDM and $f(Q, T)$ gravity models have been calculated using data from CC+BAO, Pantheon+SHOES, and a joint analysis using CC+BAO+Pantheon+SHOES. These values encompass the likelihood ($\mathcal{L}(\hat{\theta}|data)$), chi-square (χ^2), reduced chi-square (χ^2_ν), Akaike Information Criterion (AIC), the change in AIC ($|\Delta AIC|$), Bayesian Information Criterion (BIC), and the change in BIC ($|\Delta BIC|$). These statistical metrics are essential for model selection, as they provide insights into the goodness-of-fit and allow for a comparative assessment of the $f(Q, T)$ gravity models relative to the Λ CDM model, which serves as the reference model. The AIC and BIC criteria, in particular, are instrumental in determining the viability of an $f(Q, T)$ gravity model. The AIC and BIC values are calculated using the following formulas:

- $AIC = \chi^2 + 2K,$
- $BIC = \chi^2 + \kappa \log(N_i),$

14

(37)

where χ^2 is derived from the model's Gaussian likelihood function, $\mathcal{L}(\hat{\theta}|\text{data})$, and κ represents the number of free parameters in the model. N_i corresponds to the number of data points in the i -th dataset. We utilize the Jeffreys scale [59] to assess whether an $f(Q, T)$ gravity model is 'accepted' or 'rejected' in comparison to Λ CDM. On this scale, a $\Delta\text{IC} \leq 2$ denotes significant observational support, a range of $4 \leq \Delta\text{IC} \leq 7$ indicates moderate support, and $\Delta\text{IC} \geq 10$ reflects a lack of observational support. Here, ΔIC encompasses both ΔAIC and ΔBIC . We presented the statistical analysis in Table 2. Based on this analysis using the Jeffreys scale for model comparison, the $f(Q, T)$ models are not entirely ruled out but do encounter challenges in terms of observational support compared to the Λ CDM model. For the CC+BA0 dataset, the $\Delta\text{AIC} = 2.845$ indicates moderate support for the $f(Q, T)$ model, while the $\Delta\text{BIC} = 6.932$ suggests a stronger preference for Λ CDM. In the case of the Pantheon+SHOES dataset, the $\Delta\text{AIC} = 1.160$ provides moderate support for $f(Q, T)$; however, the $\Delta\text{BIC} = 8.257$ indicates a weak observational support, further suggesting that the $f(Q, T)$ model is less favored compared to Λ CDM. For the combined CC+BA0+Pantheon+SHOES datasets, the $\Delta\text{AIC} = 3.07$ signifies significant support for the $f(Q, T)$ model, but the $\Delta\text{BIC} = 7.863$ indicates less support with observation based on the Jeffrey scale, again favoring the Λ CDM model.

5. Results and Discussion

In this paper, the late-time accelerating expansion of the Universe has been investigated in the framework of $f(Q, T)$ gravity model, where Q is the non-metricity scalar and T is the trace of the energy-momentum tensor. After we reviewed, the theoretical frameworks of the background cosmology in $f(Q, T)$ gravity, a generalized paradigm model $f(Q, T) = -\alpha_0 Q - \frac{\beta_0}{H_0^2} T^2 + \eta_0$ is employed with different cosmological datasets. Using the MCMC simulation the best-fit values of different observational parameters namely $\{ \Omega_{m0}, H_0, \alpha_0, \beta_0 \}$ are constrained using the datasets CC+BA0, Pantheon+SHOES and their combination CC+BA0+Pantheon+SHOES as presented in Table 1. By taking into account the constraining values of the Hubble constant $H_0 = 73.88 \pm 1.3$, the comparison has been made with the late time and early time measurements of H_0 , see Fig. 2. Our results suggest that the $f(Q, T)$ gravity model might be contribute to a partial resolution of the Hubble tension, especially within the context of late-time cosmological observations. This partial alleviation supports the model's viability for future studies aimed at addressing the H_0 discrepancy. Using the constrained best-fit values taken from Table 1, different dynamical constraints such as the acceleration parameter $q(z)$, the effective equation of state parameter w_{eff} , the Hubble parameter $H(z)$ and the distance modulus $\mu(z)$ have been examined as presented in Figures 3 and 4 respectively, to validate the viability of the $f(Q, T)$ model against Λ CDM to explain the late time cosmic history. The numerical results of these dynamical quantities depict that the results of our considered $f(Q, T)$ gravity model align well with the expected observed cosmic acceleration and behave similarly to the Λ CDM model. The deceleration parameter towards $q \approx -0.59$ and the effective EoS parameter towards $\omega_{eff} \approx -0.72$ at redshift $z \approx 0$, such behavior reflects the Universe's approach to a quintessence phase, where the expansion is driven by a DE component that behaves like a cosmological constant. This strongly indicates the $f(Q, T)$ gravity ability to transition from decelerating expansion to accelerating expansion which is crucial for understanding the nature of late-time cosmic dynamics.

Further analysis has been conducted by considering the state finder parameters, r and s ,

to provide a deeper geometric interpretation of this model. The $r - q$ plane reveals a clear trajectory towards the Λ CDM fixed point, confirming the model's consistency with known cosmic evolution patterns. And the $r - s$ diagnostic further supports the conclusion that this $f(Q, T)$ model behaves similarly to quintessence cosmology, while also matching Λ CDM predictions in the long-term evolution. The $Om(z)$ diagnostic serves as a further independent test, showing little variation at low redshifts, which is expected in models that approach Λ CDM behavior. This reinforces the robustness of the $f(Q, T)$ gravity model in explaining the current accelerated expansion without the need for a dark energy scenario.

Finally, we conducted a detailed statistical analysis for further examining of viability $f(Q, T)$ gravity model by taking into the Λ CDM as an accepted model. Overall, we noticed that the $f(Q, T)$ models present some significant support in certain instances, especially indicated by AIC values, the BIC results consistently reflect a stronger preference for the Λ CDM model and $f(Q, T)$ models may still weak support observational based on Jeffrey's range since the AIC and BIC values are very sensitive to the number of parameters K , see Table 2. In general, the two models, $f(Q, T)$ and Λ CDM, exhibit distinct values for $\mathcal{L}(\hat{\theta}|data)$ and χ^2 . This divergence becomes worthwhile in other statistical measures, notably the AIC and BIC, due to the dependence on the number of parameters K and the dataset size N_i for each i^{th} dataset as presented in equation (37). Specifically, Λ CDM has two free parameters $\{\Omega_m, H_0\}$. In contrast, the $f(Q, T)$ model involves four parameters $\{\Omega_m, H_0, \alpha_0, \beta_0\}$, leading to substantial variation in AIC, BIC, and their respective differences, $|\Delta AIC|$ and $|\Delta BIC|$, which reflects the influence of parameter count rather than the inherent nature of the $f(Q, T)$ gravity model.

To sum up, the $f(Q, T)$ gravity model provides a viable framework for understanding the late-time accelerated expansion of the Universe without relying solely on a dark energy scenario. By using observational datasets, the model successfully captures a quintessence-like behavior and aligns with the observed transition from decelerating to accelerating cosmic phases. In particular, the ability of the $f(Q, T)$ model to approximate the Λ CDM predictions while also accounting for deviations at higher redshifts makes it a powerful alternative for overcoming persistent difficulties such as the Hubble tension. As a generalized extension of General Relativity, the $f(Q, T)$ gravity framework opens new possibilities for exploring the interactions between matter, geometry, and cosmic dynamics. With further testing against current and future high-precision cosmological observations, this model is expected to shed more light on the fundamental nature of cosmic acceleration and dark energy.

References

- [1] Riess A G *et al.* 1998 *The astronomical journal* **116** 1009
- [2] Perlmutter S *et al.* 1999 *The Astrophysical Journal* **517** 565 URL <https://dx.doi.org/10.1086/307221>
- [3] Koivisto T and Mota D F 2006 *Physical Review D—Particles, Fields, Gravitation, and Cosmology* **73** 083502
- [4] Daniel S F *et al.* 2008 *Physical Review D—Particles, Fields, Gravitation, and Cosmology* **77** 103513
- [5] Eisenstein D J *et al.* 2005 *The Astrophysical Journal* **633** 560
- [6] Caldwell R R and Doran M 2004 *Physical Review D* **69** 103517
- [7] Huang Z Y *et al.* 2006 *Journal of Cosmology and Astroparticle Physics* **2006** 013
- [8] Collaboration P, Aghanim N *et al.* 2020
- [9] Carroll S M 1998 *Physical Review Letters* **81** 3067
- [10] Fujii Y 1982 *Physical Review D* **26** 2580
- [11] Chiba T, Okabe T and Yamaguchi M 2000 *Physical Review D* **62** 023511
- [12] Armendariz-Picon *et al.* 2000 *Physical Review Letters* **85** 4438
- [13] Bento M C *et al.* 2002 *Physical Review D* **66** 043507

- [14] Kamenshchik A *et al.* 2001 *Physics Letters B* **511** 265–268
- [15] Sahlou S, Sami H, Hough R, Elmardi M, Swart A M and Abebe A 2023 *International Journal of Modern Physics D* **32** 2350090
- [16] de la Macorra A *et al.* 2011 *Phys. Rev. D* **84**(12) 121301 URL <https://link.aps.org/doi/10.1103/PhysRevD.84.121301>
- [17] Tong M and Noh H 2011 *The European Physical Journal C* **71** 1–7
- [18] Freese K *et al.* 1987 *Nuclear Physics B* **287** 797–814
- [19] Abdel-Rahman A M 1992 *Physical Review D* **45** 3497
- [20] Appleby S A and Battye R A 2007 *Physics Letters B* **654** 7–12
- [21] Amendola L *et al.* 2007 *Physical Review D—Particles, Fields, Gravitation, and Cosmology* **75** 083504
- [22] Saffari R and Rahvar S 2008 *Physical Review D—Particles, Fields, Gravitation, and Cosmology* **77** 104028
- [23] Ren X *et al.* 2021 *Physics of the Dark Universe* **32** 100812
- [24] Nashed G 2015 *General Relativity and Gravitation* **47** 1–14
- [25] Setare M and Mohammadipour N 2013 *Journal of Cosmology and Astroparticle Physics* **2013** 015
- [26] Harko T *et al.* 2011 *Physical Review D—Particles, Fields, Gravitation, and Cosmology* **84** 024020
- [27] Sahlou S, Alfedeeleb A H and Abebe A 2024 *arXiv preprint arXiv:2406.08303*
- [28] Jiménez J B *et al.* 2018 *Physical Review D* **98** 044048
- [29] Jiménez J B *et al.* 2020 *Physical Review D* **101** 103507
- [30] Xu Y, Li G *et al.* 2019 *The European Physical Journal C* **79** 1–19
- [31] Zubair M, Waheed S and Ahmad Y 2016 *The European Physical Journal C* **76** 1–13
- [32] Loo T H *et al.* 2023 *The European Physical Journal C* **83** 261
- [33] Bahamonde S and Järv L 2022 *The European Physical Journal C* **82** 1–21
- [34] Pacif S 2020 *The European Physical Journal Plus* **135** 1–34
- [35] Pacif S K J *et al.* 2017 *International Journal of Geometric Methods in Modern Physics* **14** 1750111
- [36] Zhao D 2022 *The European Physical Journal C* **82** 303
- [37] Kale A *et al.* 2023 *Symmetry* **15** 1835
- [38] Khurana M *et al.* 2024 *Physics of the Dark Universe* **43** 101408
- [39] Myrzakulov N *et al.* 2023 *Chinese Journal of Physics* **86** 300–312
- [40] Narawade S *et al.* 2023 *Nuclear Physics B* **992** 116233
- [41] Arora S and Sahoo P 2020 *Physica Scripta* **95** 095003
- [42] Bhagat R *et al.* 2023 *Physics of the Dark Universe* **42** 101358
- [43] Scolnic D M *et al.* 2018 *The Astrophysical Journal* **859** 101
- [44] Yu H *et al.* 2018 *The Astrophysical Journal* **856** 3
- [45] Dixit A *et al.* 2023 *Indian Journal of Physics* **97** 3695–3705
- [46] Aghanim N *et al.* 2020 *Astronomy & Astrophysics* **641** A6
- [47] Adame A *et al.* 2024 *arXiv preprint arXiv:2404.03002*
- [48] Park C G and Ratra B 2019 *Astrophysics and Space Science* **364** 1–10
- [49] Riess A G *et al.* 2019 *The Astrophysical Journal* **876** 85
- [50] Wong K C *et al.* 2020 *Monthly Notices of the Royal Astronomical Society* **498** 1420–1439
- [51] Riess A G *et al.* 2011 *The Astrophysical Journal* **730** 119
- [52] Foreman-Mackey o 2013 *Publications of the Astronomical Society of the Pacific* **125** 306
- [53] Hough R, Abebe A and Ferreira S 2020 *The European Physical Journal C* **80** 787
- [54] Lewis A 2019 *arXiv preprint arXiv:1910.13970*
- [55] Zhang H and Zhu Z H 2006 *Physical Review D—Particles, Fields, Gravitation, and Cosmology* **73** 043518
- [56] Li M 2004 *Physics Letters B* **603** 1–5
- [57] Sahni V *et al.* 2003 *Journal of Experimental and Theoretical Physics Letters* **77** 201–206
- [58] Sahni V, Shafieloo A and Starobinsky A A 2008 *Physical Review D—Particles, Fields, Gravitation, and Cosmology* **78** 103502
- [59] Nesseris S and Garcia-Bellido J 2013 *Journal of Cosmology and Astroparticle Physics* **2013** 036